MODELING THE PROTEIN CORONA OF GOLD NANOPARTICLES IN THE SYSTEMIC CIRCULATION

An Undergraduate Research Scholars Thesis

by

RYAN BLANCHARD

Submitted to the LAUNCH: Undergraduate Research office at
Texas A&M University
in partial fulfillment of requirements for the designation as an

UNDERGRADUATE RESEARCH SCHOLAR

Approved by
Faculty Research Advisor: Isaac Adjei

May 2021

Major: Biomedical Engineering

RESEARCH COMPLIANCE CERTIFICATION

Research activities involving the use of human subjects, vertebrate animals, and/or biohazards must be reviewed and approved by the appropriate Texas A&M University regulatory research committee (i.e., IRB, IACUC, IBC) before the activity can commence. This requirement applies to activities conducted at Texas A&M and to activities conducted at non-Texas A&M facilities or institutions. In both cases, students are responsible for working with the relevant Texas A&M research compliance program to ensure and document that all Texas A&M compliance obligations are met before the study begins.

I, Ryan Blanchard, certify that all research compliance requirements related to this Undergraduate Research Scholars thesis have been addressed with my Research Faculty Advisor prior to the collection of any data used in this final thesis submission.

This project did not require approval from the Texas A&M University Research Compliance & Biosafety office.

TABLE OF CONTENTS

ABSTRACT

Modeling the Protein Corona of Gold Nanoparticles in the Systemic Circulation

Ryan Blanchard
Department of Biomedical Engineering
Texas A&M University

Research Faculty Advisor: Dr. Isaac Adjei
Department of Biomedical Engineering
Texas A&M University

Nanoparticles (NP) adsorb layers of proteins onto their surface after systemic administration that imparts a unique identity. The protein corona formed on the NPs influences their pharmacokinetics and biodistribution, and ultimately, their drug delivery effectiveness. Thus, understanding the protein corona's role on the *in vivo* behavior of NPs is necessary to improve their efficiency as a drug delivery platform. Previous studies have indicated a difference between the protein coronas formed on NPs in static and dynamic conditions. However, the effects of the complex vascular geometry of the systemic circulation on the protein corona remain unexplored. In this study, PEGylated gold NPs (AuNP) were synthesized and the effect of different vessel geometries on the protein corona was evaluated. The AuNPs were characterized for their size (dynamic light scattering, transmission electron microscopy) and charge (zeta potential). AuNPs were exposed to plasma in loop and branched vessel configurations of a custom-built dynamic flow system, and the composition of its protein corona was compared to the protein corona on NPs under static conditions through gel electrophoresis.

These studies show that the geometry of the systemic circulation impacts the protein corona formed on NPs and could affect their in vivo behavior.

ACKNOWLEDGEMENTS

Contributors

I would like to thank my faculty advisor, Dr. Isaac Adjei, and my graduate mentor, Sridevi Conjeevaram, for their guidance and support throughout the course of this research. I would also like to thank the other members of our lab for their support.

Thanks to my colleagues, the department faculty, and staff for making my time at Texas A&M University a great experience.

Thanks to the Craig and Galen Brown Foundation for their support throughout my time at Texas A&M. Finally, thanks to my friends for their encouragement and support and to my parents for their patience and love.

The procedures used for Modeling the Protein Corona of Gold Nanoparticles in the Systemic Circulation were provided in part by Sridevi Conjeevaram. Transmission electron microscopy images depicted in Modeling the Protein Corona of Gold Nanoparticles in the Systemic Circulation were collected by Sridevi Conjeevaram and this data is unpublished.

All other work conducted for the thesis was completed by the student independently.

Funding Sources

Undergraduate research was supported by the Department of Biomedical Engineering at Texas A&M University.

No additional funding was received for this work.

NOMENCLATURE

NP	Nanoparticle
AuNP	Gold nanoparticle
PEG	Poly(ethylene glycol)
PAH	Poly(allylamine hydrochloride)
DLS	Dynamic Light Scattering
TEM	Transmission Electron Microscopy
SDS-PAGE	Sodium Dodecyl Sulfate- Polyacrylamide Gel Electrophoresis
CFD	Computational Flow Dynamics

1. INTRODUCTION

Nanotechnology, a field that has grown immensely in recent decades, utilizes cutting-edge techniques to study matter on a tiny level. Specifically, it focuses on materials in the nanometer scale, or 1×10^{-9} m. At this size, materials exhibit unique properties due to their small size and large proportion of surface atoms. Nanomaterials exhibit improved mechanical properties, enhanced optical emission, and reduced melting points, among other properties [1, 2].

The attributes of nanomaterials allow for their use in a variety of applications, particularly in medicine. Nanoparticles, defined as a particle within 1-100 nm, are used widely in biosensors, medical imaging, and delivery of therapeutics [3]. Nanoparticles hold great promise in these areas because their properties can be customized to modify how the particles interact with the patient's body [4]. One of the focal points of research interest has been focused on studying how the size, shape, surface charge, or surface chemistry of the nanoparticles affect key attributes with respect to drug delivery, such as cellular uptake and toxicity [5-7].

Upon systemic administration of the nanoparticles, layers of proteins adsorb to their surface. These proteins, referred to collectively as the protein corona, impart a unique identity onto the nanoparticle, affecting how it interacts with its environment [8]. However, the protein corona-nanoparticle complex is a dynamic system. The composition of the corona is affected by its surroundings and the amount of time in circulation [9-11]. Temporally, the composition of the corona follows the Vroman effect: when the nanoparticle first enters the systemic circulation, the corona consists mostly of proteins that are most abundant in the bloodstream. Over time, they are replaced by proteins with higher affinity for the nanoparticle.

The proteins of the corona can be separated into two categories: the hard corona and the soft corona [12]. The hard corona consists of proteins that have the highest affinity for the nanoparticle and are bound tightly to it. These ‘core’ proteins become essential to the biological identity of the nanoparticle, affecting its interactions with the environment [13, 14]. In addition, when the proteins adsorb onto the surface of the nanoparticle, their secondary and tertiary structure may be altered, influencing their function [15]. The soft corona, in contrast, consists of proteins with a relatively lower affinity for the nanoparticle [15]. Since they are more weakly bound, the proteins in this layer are constantly changing.

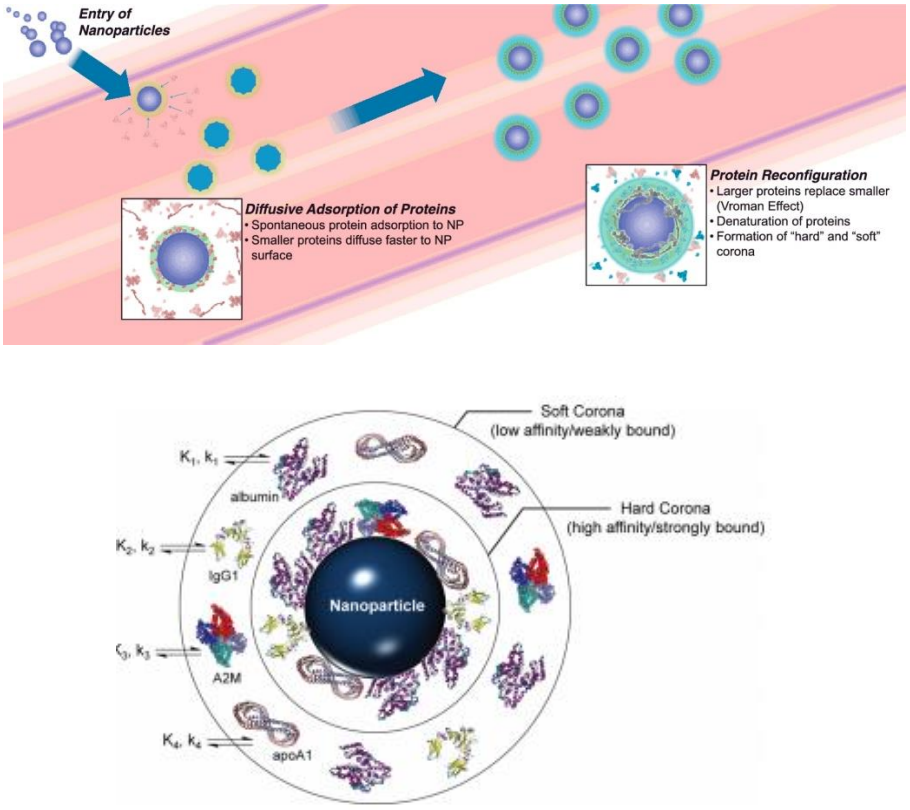

Figure 1.1: (a) As nanoparticles enter the systemic circulation, proteins adsorb to the nanoparticle. (b) The protein corona is divided into hard and soft coronas based on their affinity for the nanoparticle. Figures adapted with permission [16, 17]

Like other properties of the nanoparticle, the composition of the protein corona affects its pharmacokinetics and biodistribution [13]. Ultimately, this impacts the effectiveness of the nanoparticle as a platform for drug delivery. Therefore, it is important to understand what proteins are found in the corona, what factors affect its composition, and how these factors impact the safety and efficacy of the nanoparticles as platforms for drug delivery.

Previous studies have sought to accomplish these goals by studying how properties of interest of nanoparticles (such as size, shape, surface charge, or surface chemistry) impact the protein corona [15, 18]. These studies found, in addition, that the sample preparation procedures and incubation methods of the nanoparticles greatly influences the composition of the protein corona [19]. Yet many of these studies are performed by incubating the nanoparticles in a biological media such as human plasma under static conditions and analyzing the composition of the protein corona. The problem with this *in vitro* experimental setup is that in an *in vivo* setting, the nanoparticles will never be static as they travel through the systemic circulation.

The solution to this problem is to either utilize an *in vivo* model, which introduces many complexities and costs into a study, or to incubate the nanoparticles in circulating media, termed dynamic conditions, as shown in Figure 1.2. Multiple studies have found that, when dynamic conditions were compared to static conditions, the concentration of proteins in the corona increased and the identity of these proteins were different [20, 21]. Further, when different physiologically relevant flow speeds were selected, the composition of the protein corona varied by flow rate [20].

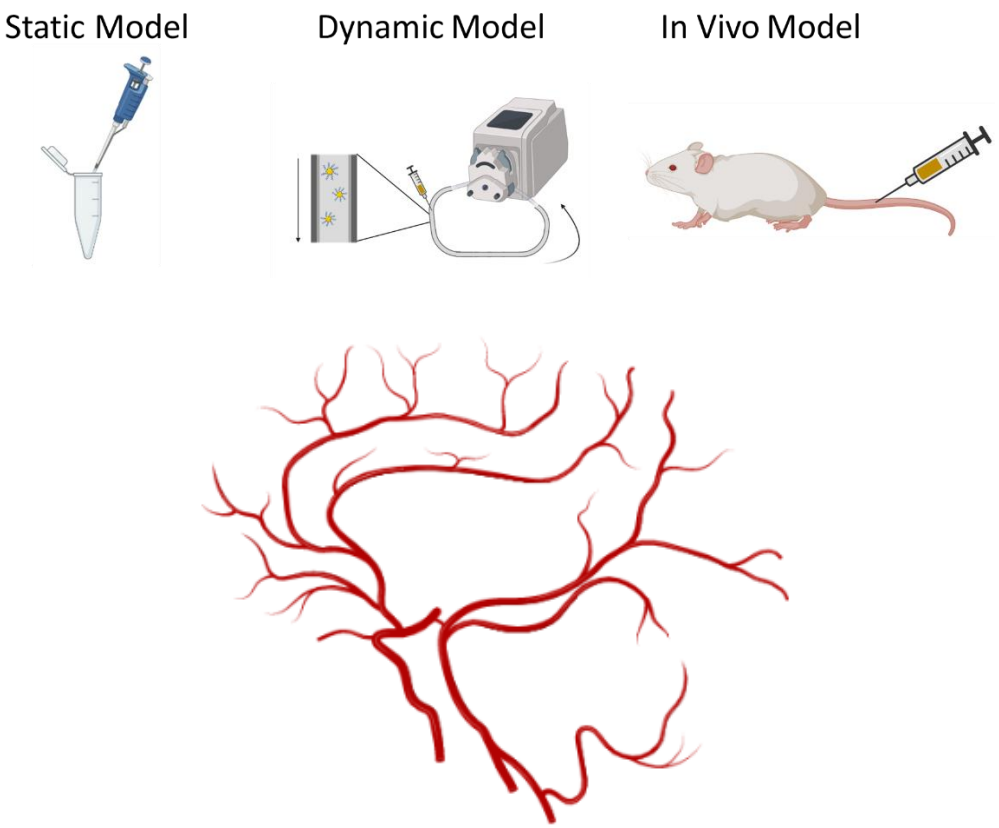

Figure 1.2: (a) Current protein corona models. (b) Blood vessels branch off one another, creating complex flow patterns.

While the dynamic conditions described will give a more accurate understanding of the protein corona that forms *in vivo* compared to static conditions, they do not take the geometry of the systemic circulation into consideration. As illustrated in Figure 1.2b, blood vessels do not proceed in a loop throughout the body like the currently used dynamic model. Rather, the anatomy of the circulatory system is branching, with variations in the vessel size and the blood flow rate. It is possible that these complexities alter the composition of the protein corona on nanoparticles. If this is the case, current *in vitro* models may need to be adjusted to ensure accurate results.

In this study, we seek to bridge the gap between current *in vitro* and *in vivo* models of the protein corona. We will investigate how altering the geometry of the flow system utilized for nanoparticle incubation will affect the composition of the protein corona. To accomplish this goal, we will design a custom-built dynamic flow system to better emulate *in vivo* conditions.

For this study, gold nanoparticles (AuNP) conjugated with poly(ethylene glycol) (PEG) will be utilized as a model nanoparticle. AuNPs were selected due to their ease of synthesis, high monodispersity, and ease of functionalization [22]. The AuNPs will be synthesized and characterized by size and charge, then they will be incubated in the flow system and the composition of their protein coronas will be analyzed.

2. METHODS

This section will detail the procedures utilized in to accomplish the results found later in this document.

2.1 AuNP Synthesis

The first step in the process is producing AuNP. First, a 25mM stock solution of the gold precursor tetrachloroauric(III) acid trihydrate ($HAuCl_4 \cdot 3H_2O$) is prepared and stored at 8°C. The stock solution was then diluted to a 10mM solution. 1.25 mL of 10mM $HAuCl_4 \cdot 3H_2O$ was added to 100 mL of deionized (DI) water in a conical flask. This flask was placed on a magnetic stirring hot plate in a fume hood, measuring the temperature of the solution while heating. When the temperature reached 70°C, 1 mL of 1.5 mg/mL poly(allylamine) hydrochloride (PAH), a cationic polyelectrolyte, is added. Once the solution reached 100°C, the reduction reaction was allowed to continue for 20 minutes until the solution turned a deep red color. The solution was cooled to room temperature, and 1 mg of 10 kDa thiol-(poly)ethylene glycol-amine (SH-PEG-NH_2) was added and stirred for one hour to incorporate. PEG serves to prevent the formed AuNP from aggregating through steric hindrance. The solution was split into two 50 mL centrifuge tubes and transferred to an ultracentrifuge at 4000 RPM for 30 minutes. The supernatant was decanted, and the pellet transferred to a 1.5 mL centrifuge tube. The pellet was then centrifuged at 14,800 RPM for 15 minutes, and any remaining supernatant was decanted and discarded into a chemical waste container. The pellet, or the completed AuNP, was then stored at 8°C until the experiment. Glassware was cleaned with aqua regia, which consists of a 1:3 ratio of concentrated HCl and HNO_3.

2.2 AuNP Characterization

To ensure that AuNP were consistent within and between batches, particles were characterized by charge and size.

2.2.1 Zeta Potential

To characterize the charge of the nanoparticles, the zeta potential was measured using the Malvern Zetasizer Nano ZS. Zeta potential is defined as the electric potential difference between the layer of ions bound strongly to the AuNP and the layer of oppositely-charged ions in the surrounding dispersion medium [23]. This measurement is useful because zeta potential is an important indicator of stability [24]. A higher magnitude of zeta potential indicates that the nanoparticles are more stable and thus less likely to aggregate. In addition, a positive zeta potential was sought to confirm successful reduction of AuNP by PAH.

To obtain the measurement, 200 μL of AuNP were diluted 1:5. Using a 1 mL tuberculin syringe, the nanoparticles are injected into a folded capillary zeta cell to the fill line. The cell is then inspected to ensure there are no air bubbles inside the cell, as this will disrupt the reading. The cell is capped, and the nanoparticles can be measured.

2.2.2 Dynamic Light Scattering (DLS)

AuNP size was determined utilizing several techniques. The first method is dynamic light scattering, which is measured using the Malvern Zetasizer Nano ZS. Dynamic light scattering measures the uses the fluctuation of scattered light intensity to estimate the Brownian motion of the nanoparticles, which can be used to calculate its hydrodynamic diameter [25]. The hydrodynamic diameter reflects the size of a theoretical solid sphere that would diffuse the same as the particle measured. These measurements produce a Z-average, or intensity weighted mean

hydrodynamic diameter, and a polydispersity index (PDI), which is a measure of the variation of size within the distribution.

2.2.3 UV-VIS Spectroscopy

UV-VIS spectroscopy is a useful technique to confirm AuNP size and to determine the concentration of nanoparticles in solution [26]. This is accomplished by obtaining an absorption spectrum of the sample in the UV and visual light spectra. To perform the reading, 100 μL of 1:5 dilution AuNP are added to a 96-well plate. The plate is then read using the Tecan Infinite M200 Pro Plate Reader. For 20 nm diameter AuNP, the absorption peak will be located at 530 nm. To obtain the concentration of AuNP, the absorption at 530 nm is recorded. Using the Beer-Lambert law and the dilution factor, the concentration of AuNP in nanoparticles/mL can be obtained.

2.2.4 Transmission Electron Microscopy (TEM)

TEM utilizes an electron beam transmitted through a sample to produce a high-resolution image. AuNP were dispersed in ethanol and sonicated to mix. A single drop of the AuNP-ethanol solution was added onto a copper grid and dried under vacuum. The images are taken using the JEOL 1200EX microscope. TEM is useful for analyzing the size distribution and morphology of nanoparticles [27]. To find the size distribution of AuNP, image analysis software is used. The image is imported into ImageJ, where the image is processed and particle analysis is performed. This analysis produces a distribution of particle diameter. It should be noted that this diameter is not equivalent to the hydrodynamic diameter calculated from DLS, as this diameter is based on the visual reference of the nanoparticle rather than the motion of the nanoparticle in solution.

2.3 Design of Custom Dynamic Flow System

2.3.1 General Design

The dynamic flow system consisted of a Fisherbrand™ Variable-Flow Peristaltic Pumps and varying lengths of polyurethane tubing. The system was placed in a temperature-controlled orbital shaker maintaining 37°C. Two primary configurations were utilized for this study. The loop configuration, shown in Figure 2.1a, consisted of a single length of tubing connected to both ends of the peristaltic pump. The branching configuration, as shown in Figure 2.1b, consisted of four lengths of tubing. Two segments connected to each end of the peristaltic pump and two segments were connected in between using polypropylene Y fittings.

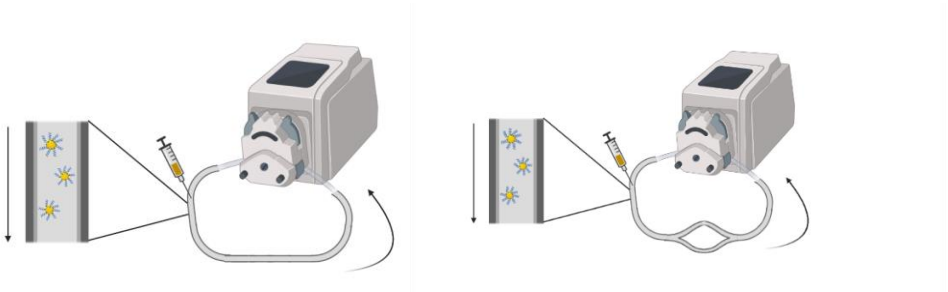

Figure 2.1: Design of custom dynamic flow system. (a) Loop configuration (b) Branched configuration.

2.3.2 First Flow System Iteration

In the first iteration, 1/16” inner diameter (ID) tubing was utilized. The tubing length for the loop configuration was 8”. The tubing lengths for the branched configuration was 2” for each segment. This loop configuration was utilized in both Section 3.2 and Section 3.3.1. For the first iteration trials described in Section 3.3.1, the flow rate was 5.2 mL/min.

2.3.3 Second Flow System Iteration

In the second iteration, 3/32” ID tubing was utilized. The tubing length for the loop configuration was 16”. The segments for the branched configuration were each 4”. The flow rate for this iteration was 5.2 mL/min.

2.3.4 Third Flow System Iteration

In the third iteration, the tubing length remains the same as described in section 2.4.3. The loop configuration and the ends of the branched configuration used 3/32” ID tubing, while the branches used 1/16” ID tubing. The flow rate for this iteration was 9.3 mL/min.

2.4 Protein Corona Formation and Analysis

2.4.1 General Experimental Protocol

Thawed human plasma was first filtered through a 0.22 μm syringe filter and warmed in a water bath. The pump was filled with warmed plasma and was circulated at a speed specific to the experiment. 50 μL of 1×10^{11} NP/mL AuNP were injected into the circulating plasma using an insulin syringe. At the same time, 50 μL of the same concentration of AuNP was added to a static container of plasma within the shaker to serve as a control. The nanoparticles interacted with the plasma for 10 minutes before being removed and placed in a centrifuge tube. The AuNP-plasma solution was centrifuged thrice, replacing the removed supernatant with phosphate-buffered saline (PBS). After the washing, the pellet was collected and stored at 4°C

for analysis. To confirm results, each set of experiments was repeated thrice.

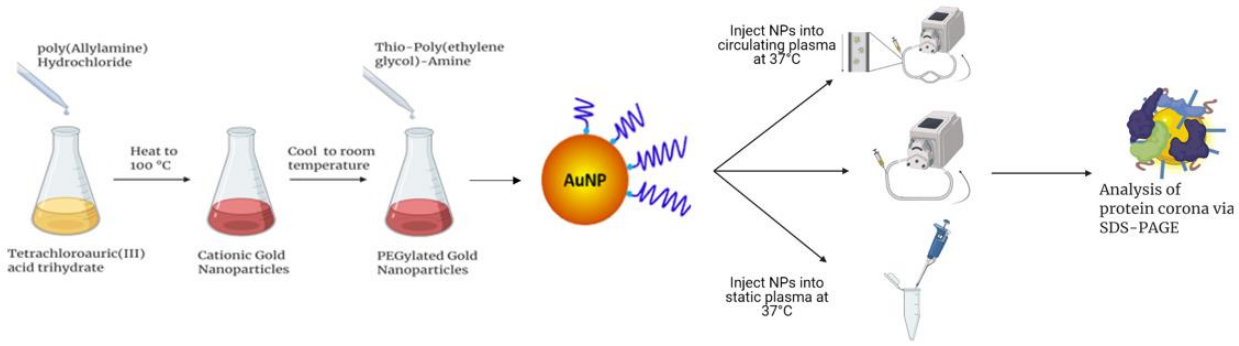

Figure 2.2: Experiment overview.

2.4.2 SDS-PAGE

To analyze the composition of the protein corona, sodium dodecyl sulfate polyacrylamide gel electrophoresis (SDS-PAGE) was utilized. SDS-PAGE separates proteins in a sample based on their molecular weight. SDS, an ionic detergent, denatures the protein structure and coats the protein backbone with a negative charge. An electric field draws the denatured proteins through the polyacrylamide gel, travelling at a rate proportional to its molecular weight.

Hand-cast stain-free polyacrylamide gels were synthesized within one week of the experiment using the Bio-Rad Mini-PROTEAN Tetra Handcast System, following manufacturer instructions. The synthesized gel was stored at 4°C wrapped in a paper towel wetted with SDS-PAGE running buffer **(**Tris/glycine/SDS**)** that has been diluted from 10X to 1X. Once the protein pellet had been collected as per the experiment outlined in Section 2.4.1, the components of the electrophoresis setup were rinsed with DI water and the gel was removed from storage. The gel and a buffer dam were loaded into the electrophoresis chamber, which was then filled with running buffer until the two-gel line on the chamber side.

5 µL of 4X Laemeli sample buffer was added to each pellet and diluted with 15 µL of 2% SDS to create 20 µL of 1X Laemeli sample buffer. The samples were transferred to a centrifuge

tube holder, which was placed in a water bath. This water bath was microwaved for 3 minutes. The samples were removed from the water bath and cooled to room temperature. They were placed into the centrifuge, which was pulsed for 30 seconds to pellet any debris. The comb was removed carefully from the gel and 20 μL of supernatant was injected into each lane. The first lane was saved to inject 5 μL of Bio-Rad Precision Plus Protein™ Dual Color Standard. The lid was placed on the chamber and the device was run for about one hour, or until the dye front reaches the bottom, at 110 V, checking periodically. Using DI water and a gel releaser, the gel was removed from the plates and transferred to a sample tray. The tray was inserted into the Bio-Rad Gel Doc EZ Imager, which imaged the gel.

3. RESULTS

3.1 AuNP Synthesis

To synthesize AuNP, chloroauric acid is reduced in DI water by PAH. The resulting neutral gold atoms form nuclei, which grow into AuNP, as shown in Figure 3.1. By controlling the feed rate and ratios, the size of the nanoparticle can be controlled [28]. However, these AuNP are not stable in aqueous environments over long periods of time, so they must be either sterically or ionically stabilized [29]. To accomplish this, SH-PEG-NH_2 is conjugated to the AuNP through a covalent bond between the thiol group and the AuNP surface [30]. Through the PEG and amine groups, this conjugation both sterically and ionically stabilizes the AuNP.

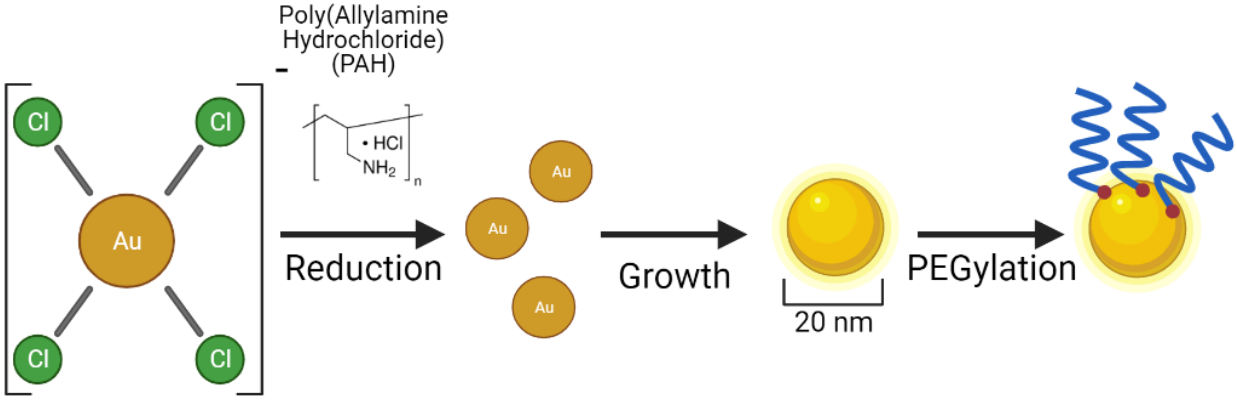

Figure 3.1: AuNP Synthesis.

3.2 AuNP Characterization

AuNP were characterized by both charge and size. The zeta potential of the AuNP was found to be 45 mV before PEG conjugation and 37.1±5.35 mV after PEG conjugation. The UV-VIS absorption scan can be seen in Figure 3.2a, which has a peak at 530 nm. This peak was consistent across all AuNP samples. Using the TEM images, shown in Figure 3.2b, the mean and

PDI of the AuNP were found to be 18.7 nm and 0.106, respectively. Finally, the hydrodynamic diameter of the AuNP, calculated using DLS, was 45 nm.

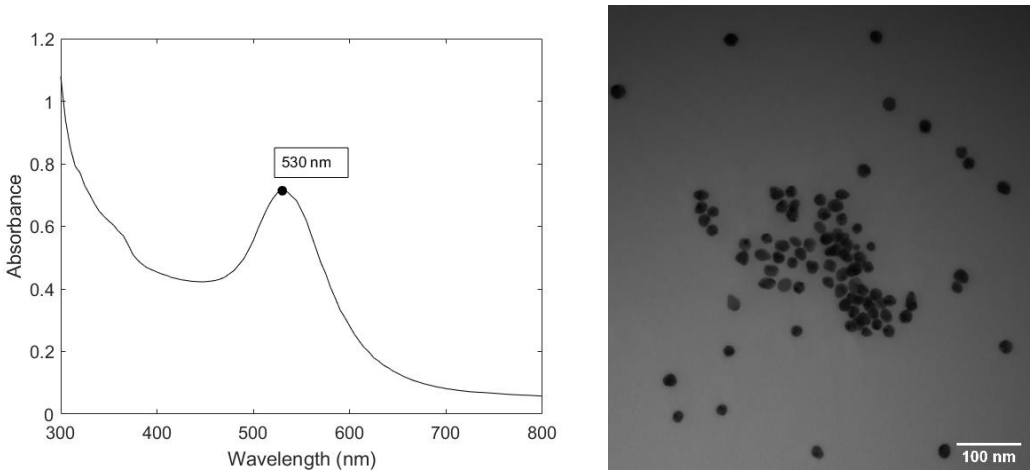

Figure 3.2: AuNP Characterization. (a) UV-VIS absorbance scan (b) TEM image

PEG conjugation is confirmed by the change in zeta potential before and after conjugation. A large magnitude of zeta potential indicates that there is sufficient surface charge repulsion for nanoparticle stabilization [31]. A positive surface charge is potentially beneficial for AuNPs as drug delivery platforms, as it leads to greater cell uptake because of the negative surface charge of the cell membrane [32]. This makes the choice of SH-PEG-NH_2 as a stabilizing agent ideal, as it creates a relevant AuNP model on which to analyze protein corona composition for drug delivery.

The difference between the diameters found through image analysis and DLS is to be expected, as they are not measuring the same parameter. AuNP velocity could be impacted by PEG conjugation, causing a relative increase in the hydrodynamic diameter[33]. Taken together, this data indicates that gold nanoparticles were successfully synthesized with PEG conjugation. These AuNP were stable, indicated by a lack of change of the absorbance peak over time, and highly monodisperse, as shown by the PDI from TEM image analysis.

3.3 Dynamic Protein Composition

The looped dynamic condition was performed at two different flow rates: 5.2 mL/min and 9.3 mL/min. The results from gel electrophoresis are shown in Figure 3.3b. When compared to a static condition the protein coronas of the dynamic conditions were different. Further, each flow rate presented differences in protein composition. This confirms findings in previous studies that incubating NP in dynamic conditions and changing the flow rate results in a difference in the composition of the protein corona [20].

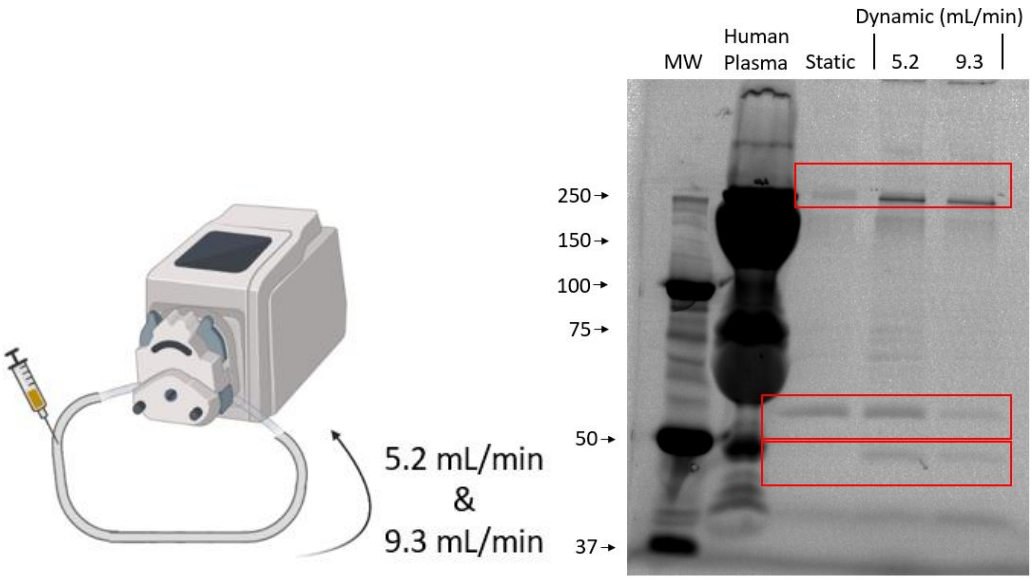

Figure 3.3: (a) AuNPs were incubated at two flow rates. (b) Relative concentrations of proteins in static and dynamic conditions found through gel electrophoresis.

3.4 Branched Protein Composition

3.4.1 First Iteration of Branched System

After establishing a connection between flow rate and protein composition, we moved onto creating the branched system to replicate the geometry of the systemic circulation. The design of this system is described in Section 2.3.2. The results from this study are shown in Figure 3.4a. This system yielded inconsistent results between trials. To investigate, water was

dyed with food coloring and circulated through the system. This test revealed that, due to a sharp turn before the branching, flow was being favored through one branch at a time, as illustrated in Figure 3.4b. Because of this, one branch was often brought to a halt. This led to inconsistencies in protein corona composition.

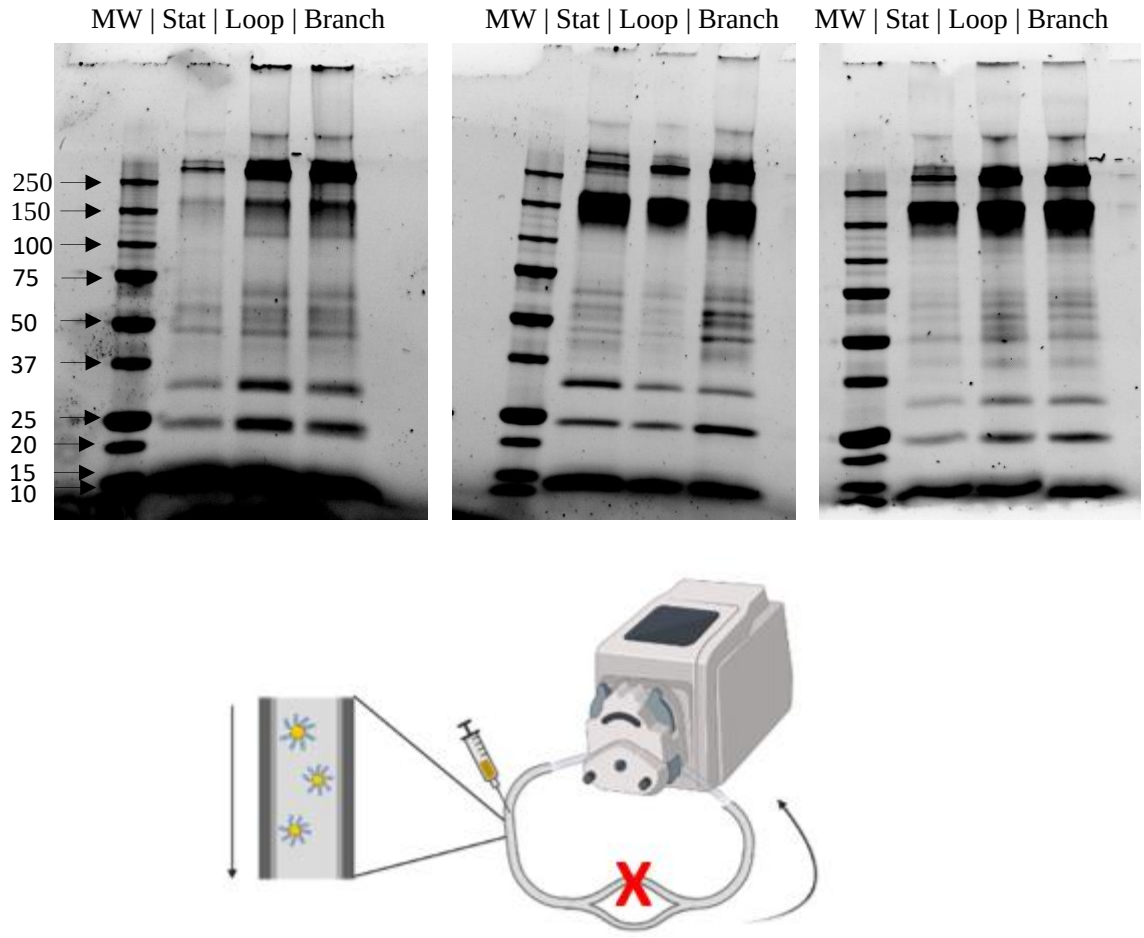

Figure 3.4: (a) Relative concentrations of proteins in static, dynamic, and branched conditions found through gel electrophoresis in the first iteration of branched geometry system. (b) In the first iteration of branched geometry system, flow was favored through one branch.

3.4.2 Second Iteration of Branched System

To rectify the issues described, both the segment length and diameter were increased. The system was then modified to the design described in Section 2.3.3. The length and diameter of the branches was increased, as seen in Figure 3.5a. The results from this study are displayed in

Figure 3.5b. When dyed water was circulated through the flow setup, it traveled through both branches evenly and consistently. However, this system did not reveal a difference between the dynamic and branched configuration. Therefore, we hypothesized that the system was still not accurately representing the systemic circulation.

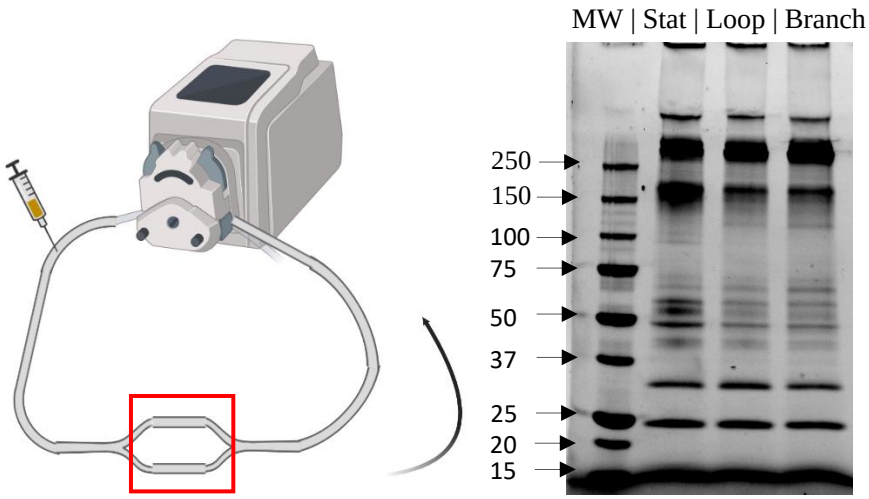

Figure 3.5: (a) In the second iteration of branched geometry system, branch length and diameter were increased. (b) Relative concentrations of proteins in static, dynamic, and branched conditions found through gel electrophoresis in the second iteration of branched geometry system.

3.4.3 Third Iteration of Branched System

In the systemic circulation, the diameter of blood vessels varies, as shown in Figure 1.2b. The diameter decreases as blood flows from the aorta to the capillaries and increases from the capillaries to the veins. In the third iteration, inspiration was taken from this anatomy by decreasing the diameter of the branching segments, illustrated in Figure 3.6a. Thus, the system was revised as described in Section 2.3.4. The results from this study are shown in Figure 3.6b. This study showed that there are multiple proteins that are not present in the loop configuration that are seen in the branched configuration. This indicates that there is a difference in the protein corona composition between AuNP incubated in dynamic systems with different configurations.

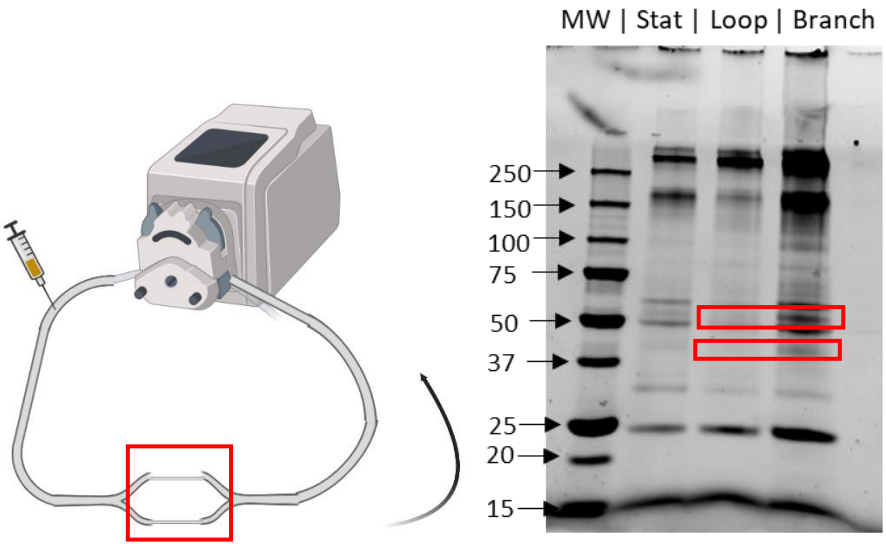

Figure 3.6: (a) In the third iteration of branched geometry system, branch diameter was decreased. (b) Relative concentrations of proteins in static, dynamic, and branched conditions found through gel electrophoresis in the third iteration of branched geometry system.

4. CONCLUSION

In this study, PEGylated AuNP were synthesized and characterized by size and charge. A dynamic flow system was constructed to model the protein corona of AuNP in the systemic circulation. Using this system, AuNP were incubated with human plasma in the looped configuration, representing the traditional 'dynamic' system, and the branched configuration, intended to be a more accurate model of the systemic circulation. This study found that there is a difference between the compositions of the protein corona formed on AuNP using looped and branched configurations.

Since the protein corona influences how nanoparticles interact with their surroundings, a change in its composition could have a major impact on nanoparticle behavior *in vivo*. To maximize the ability to translate research from the benchtop to the clinic, it is vital to create *in vitro* testing systems that reflect conditions found *in vivo* as accurately as possible. This study suggests that the current dynamic model of the protein corona *in vitro* may not fully reflect its formation *in vivo*. Thus, these findings are important because they can facilitate the effective development of nanoparticle platforms for biomedical applications.

In future studies, the impact of flow geometry on the uptake of AuNP will be examined using the configurations described above. In addition, proteins affected by geometry in dynamic flow will be identified for analysis using mass spectrometry. Lastly, a computation fluid dynamics (CFD) model of the configurations will be developed to examine how forces such as fluid shear stress vary within and between the flow configurations.

REFERENCES

[1] J. Sun and S. L. Simon, "The melting behavior of aluminum nanoparticles," *Thermochimica Acta,* vol. 463, no. 1, pp. 32-40, 2007/10/25/ 2007, doi: https://doi.org/10.1016/j.tca.2007.07.007.

[2] P. Kumbhakar, S. S. Ray, and A. L. Stepanov, "Optical Properties of Nanoparticles and Nanocomposites," *Journal of Nanomaterials,* vol. 2014, p. 181365, 2014/04/13 2014, doi: 10.1155/2014/181365.

[3] J. K. Patra *et al.*, "Nano based drug delivery systems: recent developments and future prospects," *Journal of Nanobiotechnology,* vol. 16, no. 1, p. 71, 2018/09/19 2018, doi: 10.1186/s12951-018-0392-8.

[4] M. J. Mitchell, M. M. Billingsley, R. M. Haley, M. E. Wechsler, N. A. Peppas, and R. Langer, "Engineering precision nanoparticles for drug delivery," *Nature Reviews Drug Discovery*, 2020/12/04 2020, doi: 10.1038/s41573-020-0090-8.

[5] A. Albanese, P. S. Tang, and W. C. W. Chan, "The Effect of Nanoparticle Size, Shape, and Surface Chemistry on Biological Systems," *Annual Review of Biomedical Engineering*, vol. 14, no. 1, pp. 1-16, 2012, doi: 10.1146/annurev-bioeng-071811-150124.

[6] A. Banerjee, J. Qi, R. Gogoi, J. Wong, and S. Mitragotri, "Role of nanoparticle size, shape and surface chemistry in oral drug delivery," (in eng), *J Control Release,* vol. 238, pp. 176-185, Sep 28 2016, doi: 10.1016/j.jconrel.2016.07.051.

[7] E. Fröhlich, "The role of surface charge in cellular uptake and cytotoxicity of medical nanoparticles," (in eng), *Int J Nanomedicine,* vol. 7, pp. 5577-5591, 2012, doi: 10.2147/IJN.S36111.

[8] V. H. Nguyen and B. J. Lee, "Protein corona: a new approach for nanomedicine design," (in eng), *Int J Nanomedicine,* vol. 12, pp. 3137-3151, 2017, doi: 10.2147/ijn.S129300.

[9] S. Angioletti-Uberti, M. Ballauff, and J. Dzubiella, "Competitive adsorption of multiple proteins to nanoparticles: the Vroman effect revisited," *Molecular Physics,* vol. 116, no. 21-22, pp. 3154-3163, 2018/11/17 2018, doi: 10.1080/00268976.2018.1467056.

[10] A. Cox *et al.*, "Evolution of Nanoparticle Protein Corona across the Blood–Brain Barrier," *ACS Nano*, vol. 12, no. 7, pp. 7292-7300, 2018/07/24 2018, doi: 10.1021/acsnano.8b03500.

[11] S. Prakash and R. Deswal, "Analysis of temporally evolved nanoparticle-protein corona highlighted the potential ability of gold nanoparticles to stably interact with proteins and influence the major biochemical pathways in Brassica juncea," *Plant Physiology and Biochemistry*, vol. 146, pp. 143-156, 2020/01/01/ 2020, doi: https://doi.org/10.1016/j.plaphy.2019.10.036.

[12] H. Mohammad-Beigi *et al.*, "Mapping and identification of soft corona proteins at nanoparticles and their impact on cellular association," *Nat. Commun.*, vol. 11, no. 1, p. 4535, 2020/09/10 2020, doi: 10.1038/s41467-020-18237-7.

[13] S. Ritz *et al.*, "Protein Corona of Nanoparticles: Distinct Proteins Regulate the Cellular Uptake," *Biomacromolecules*, vol. 16, no. 4, pp. 1311-1321, 2015/04/13 2015, doi: 10.1021/acs.biomac.5b00108.

[14] M. P. Monopoli, C. Åberg, A. Salvati, and K. A. Dawson, "Biomolecular coronas provide the biological identity of nanosized materials," *Nature Nanotechnology*, vol. 7, no. 12, pp. 779-786, 2012/12/01 2012, doi: 10.1038/nnano.2012.207.

[15] J. Wang *et al.*, "Soft Interactions at Nanoparticles Alter Protein Function and Conformation in a Size Dependent Manner," *Nano Letters*, vol. 11, no. 11, pp. 4985-4991, 2011/11/09 2011, doi: 10.1021/nl202940k.

[16] C. C. Fleischer and C. K. Payne, "Nanoparticle–Cell Interactions: Molecular Structure of the Protein Corona and Cellular Outcomes," *Accounts of Chemical Research*, vol. 47, no. 8, pp. 2651-2659, 2014/08/19 2014, doi: 10.1021/ar500190q.

[17] V. P. Zhdanov and N.-J. Cho, "Kinetics of the formation of a protein corona around nanoparticles," *Mathematical Biosciences*, vol. 282, pp. 82-90, 2016/12/01/ 2016, doi: https://doi.org/10.1016/j.mbs.2016.09.018.

[18] M. Lundqvist, J. Stigler, G. Elia, I. Lynch, T. Cedervall, and K. A. Dawson, "Nanoparticle size and surface properties determine the protein corona with possible implications for biological impacts," *Proceedings of the National Academy of Sciences*, vol. 105, no. 38, pp. 14265-14270, 2008, doi: 10.1073/pnas.0805135105.

[19] S. Winzen *et al.*, "Complementary analysis of the hard and soft protein corona: sample

preparation critically effects corona composition," *Nanoscale*, 10.1039/C4NR05982D vol. 7, no. 7, pp. 2992-3001, 2015, doi: 10.1039/C4NR05982D.

[20] D. T. Jayaram, S. M. Pustulka, R. G. Mannino, W. A. Lam, and C. K. Payne, "Protein Corona in Response to Flow: Effect on Protein Concentration and Structure," *Biophysical Journal*, vol. 115, no. 2, pp. 209-216, 2018, doi: 10.1016/j.bpj.2018.02.036.

[21] N. J. Braun, M. C. DeBrosse, S. M. Hussain, and K. K. Comfort, "Modification of the protein corona–nanoparticle complex by physiological factors," *Materials Science and Engineering: C*, vol. 64, pp. 34-42, 2016/07/01/ 2016, doi: https://doi.org/10.1016/j.msec.2016.03.059.

[22] R. Arvizo, R. Bhattacharya, and P. Mukherjee, "Gold nanoparticles: opportunities and challenges in nanomedicine," (in eng), *Expert Opin Drug Deliv*, vol. 7, no. 6, pp. 753-63, Jun 2010, doi: 10.1517/17425241003777010.

[23] A. A. Barba, S. Bochicchio, A. Dalmoro, D. Caccavo, S. Cascone, and G. Lamberti, "Chapter 10 - Polymeric and lipid-based systems for controlled drug release: an engineering point of view," in *Nanomaterials for Drug Delivery and Therapy*, A. M. Grumezescu Ed.: William Andrew Publishing, 2019, pp. 267-304.

[24] Y. Zhang *et al.*, "Sodium dodecyl sulfate improved stability and transdermal delivery of salidroside-encapsulated niosomes via effects on zeta potential," *International Journal of Pharmaceutics*, vol. 580, p. 119183, 2020/04/30/ 2020, doi: https://doi.org/10.1016/j.ijpharm.2020.119183.

[25] J. Coe *et al.*, "Chapter Twenty-Two - Crystallization of Photosystem II for Time-Resolved Structural Studies Using an X-ray Free Electron Laser," in *Methods in Enzymology*, vol. 557, A. K. Shukla Ed.: Academic Press, 2015, pp. 459-482.

[26] V. Amendola and M. Meneghetti, "Size Evaluation of Gold Nanoparticles by UV−vis Spectroscopy," *The Journal of Physical Chemistry C*, vol. 113, no. 11, pp. 4277-4285, 2009/03/19 2009, doi: 10.1021/jp8082425.

[27] D. J. Smith, "Chapter 1 Characterization of Nanomaterials Using Transmission Electron Microscopy," in *Nanocharacterisation (2)*: The Royal Society of Chemistry, 2015, pp. 1-29.

[28] K. Saha, S. S. Agasti, C. Kim, X. Li, and V. M. Rotello, "Gold nanoparticles in chemical and biological sensing," (in eng), *Chem Rev*, vol. 112, no. 5, pp. 2739-2779, 2012, doi:

10.1021/cr2001178.

[29] M. Sokolsky-Papkov and A. Kabanov, "Synthesis of Well-Defined Gold Nanoparticles Using Pluronic: The Role of Radicals and Surfactants in Nanoparticles Formation," (in eng), *Polymers*, vol. 11, no. 10, p. 1553, 2019, doi: 10.3390/polym11101553.

[30] J. Gao, X. Huang, H. Liu, F. Zan, and J. Ren, "Colloidal Stability of Gold Nanoparticles Modified with Thiol Compounds: Bioconjugation and Application in Cancer Cell Imaging," *Langmuir*, vol. 28, no. 9, pp. 4464-4471, 2012/03/06 2012, doi: 10.1021/la204289k.

[31] E. Joseph and G. Singhvi, "Chapter 4 - Multifunctional nanocrystals for cancer therapy: a potential nanocarrier," in *Nanomaterials for Drug Delivery and Therapy*, A. M. Grumezescu Ed.: William Andrew Publishing, 2019, pp. 91-116.

[32] P. Foroozandeh and A. A. Aziz, "Insight into Cellular Uptake and Intracellular Trafficking of Nanoparticles," (in eng), *Nanoscale Res Lett*, vol. 13, no. 1, pp. 339-339, 2018, doi: 10.1186/s11671-018-2728-6.

[33] C. M. Maguire, M. Rösslein, P. Wick, and A. Prina-Mello, "Characterisation of particles in solution - a perspective on light scattering and comparative technologies," (in eng), *Sci Technol Adv Mater*, vol. 19, no. 1, pp. 732-745, 2018, doi: 10.1080/14686996.2018.1517587.

APPENDIX: PERMISSION STATEMENTS

4.1 Figure 1a

ELSEVIER LICENSE

TERMS AND CONDITIONS

Apr 09, 2021

This Agreement between Texas A&M University -- Ryan Blanchard ("You") and Elsevier ("Elsevier") consists of your license details and the terms and conditions provided by Elsevier and Copyright Clearance Center.

License Number	5042750320277
License date	Apr 05, 2021
Licensed Content Publisher	Elsevier
Licensed Content Publication	Mathematical Biosciences
Licensed Content Title	Kinetics of the formation of a protein corona around nanoparticles
Licensed Content Author	Vladimir P. Zhdanov,Nam-Joon Cho
Licensed Content Date	Dec 1, 2016

Licensed Content Volume	282
Licensed Content Issue	n/a
Licensed Content Pages	9
Start Page	82
End Page	90
Type of Use	reuse in a thesis/dissertation
Portion	figures/tables/illustrations
Number of figures/tables/illustrations	1
Format	electronic
Are you the author of this Elsevier article?	No
Will you be translating?	No

Title	Modeling the Protein Corona of Gold Nanoparticles in the Systemic Circulation
Institution name	Texas A&M University, Department of Biomedical Engineering
Expected presentation date	Apr 2021
Portions	Graphical abstract figure

4.2 Figure 1b

Dear Mr. Blanchard,

Thank you for contacting ACS Publications Support.

Your permission requested is granted and there is no fee for this reuse. In your planned reuse, you must cite the ACS article as the source, add this direct link https://pubs.acs.org/doi/10.1021/ar500190q, and include a notice to readers that further permissions related to the material excerpted should be directed to the ACS.

If you need further assistance, please let me know.

Thank you,

Ranjith Alexander

ACS Customer Services & Information